ACADEMIC PRESS

Available at WWW.MATHEMATICSWEB.ORG POWERED BY SCIENCE @ DIRECT®

J. Math. Anal. Appl. 279 (2003) 398–417

Journal of MATHEMATICAL ANALYSIS AND APPLICATIONS

www.elsevier.com/locate/jmaa

Enhanced and restored signals as a generalized solution for shock filter models. Part II—numerical study

M. Cheriet * and L. Remaki

Imagery, Vision and Artificial Intelligence Laboratory, École de Technologie Supérieure, 1100 Notre-Dame West, Montreal, PQ H3C 1K3, Canada

Received 18 December 2000

Submitted by P. Broadbridge

Abstract

In Part I of this paper, we proposed a well-posed generalized model for signal enhancement and restoration based on shock filters. A theoretical study of the Cauchy problem in the framework of generalized functions algebra was developed in detail. In Part II, we investigate the numerical aspects of the model. We derive an efficient, explicit numerical scheme in both one and two dimensions, and investigate the schemes' stability and convergence. Through experimental tests, we demonstrate the effectiveness of the numerical schemes when restoring and enhancing signals in various situations with a limited number of iterations. Moreover, we show the impact of the coefficients introduced in the model on the procedure's processing time.

Keywords: Generalized functions; Numerical schemes; Signal enhancement and restoration; Partial differential equations (PDEs); Shock filters

1. Introduction

Approaches based on partial differential equations (PDEs) have been used extensively in the image enhancement and restoration process, providing a highly interesting formulation and interpretation of the phenomena. In Part I of this paper, in keeping with the idea first proposed by Rudin in [7,10], then improved by Alvarez et al. in [1], and later again by

* Corresponding author.
E-mail addresses: cheriet@gpa.etsmtl.ca (M. Cheriet), remaki@cfdlab.mcgill.ca (L. Remaki).

0022-247X/03/$ – see front matter
doi:10.1016/S0022-247X(02)00714-X

Alvarez and Mazorra in [2], we proposed a generalized model in the one- and two-dimensional cases in order to enhance the efficiency of the original model and enable a wider range of degrees of freedom when handling the model parameters (coefficients). After interpreting the model (as in [3,8]) within the framework of the generalized functions algebra introduced by Colombeau [4] (this theory is summarized in Part I), a theoretical study was developed in Part I proving an existence and uniqueness result and consequently the well-posedness of the proposed model. In this paper, an effective numerical scheme will be derived in both cases (one- and two-dimensional), and the scheme's stability and convergence results will be proved.

In Section 2, we review the model proposed in Part I. In Section 3, we detail the construction of the numerical scheme in one dimension. In addition, we give a series of tests to demonstrate the effectiveness of the scheme, as well as the modified model parameters' ability to positively influence processing time. In Section 4, we derive the numerical scheme in two dimensions (images) and present stability and convergence results. We conclude by exploring an application to restore and enhance synthetic and real scene images with added noise, as well as real images without added simulated noise.

2. Overview of the proposed model

We begin this section by giving an overview of the previous shock filter models that motivated our work. We then recall the proposed model developed in Part I of this paper.

2.1. Previous works

Rudin in [10] was the first to apply the concepts and techniques of the non-linear hyperbolic equation field to image enhancement. He proposed the following model:

$$u_t + F(u_{xx})|u_x| = 0 \quad \text{in } \mathbb{R} \times \mathbb{R}^+,$$

where $F(\cdot)$ is a function such that $F(s)s \geqslant 0$. To discretize this equation, an explicit monotone scheme is used, thereby preserving the total variation. As noted in [2], this scheme cannot remove certain kinds of noise, such as "salt and pepper" noise. Rudin's model generates a great number of spurious shocks at the Laplacian zero-crossings due to the influence of noise. In order to avoid these spurious shocks, Alvarez and Mazorra [2] proposed the following improved hyperbolic partial differential model, which follows the classical theory of Marr [6]:

$$u_t + F(G_\sigma * u_{xx}, G_\sigma * u_x)u_x = 0 \quad \text{in } \mathbb{R} \times \mathbb{R}^+,$$

where $G_\sigma(\cdot)$ is a smoothing kernel, and F satisfies the condition cited above. Alvarez and Mazorra developed an interesting, implicit, unconditionally-stable scheme. Initially developed by the authors in [1], this model is generalized to the case of two-dimensional signals in keeping with the directional smoothing ideas mentioned in the introduction. They propose the following parabolic–hyperbolic equation:

$$u_t = CL(u) - u_\eta F(G_\sigma * u_{\eta\eta}, G_\sigma * u_\eta) \quad \text{in } \mathbb{R}^2 \times \mathbb{R}^+,$$

where $\eta = \eta(x, y)$ represents the direction perpendicular to the gradient $\nabla u(x, y)$, C is any positive constant, and $L(u)$ is any directional smoothing operator. This model yields satisfactory results, as shown in [2]. However, to give a larger scope of application to the models derived from a shock filter theory, we believe it is necessary to maintain heightened control of the created shocks' velocity. In the models cited previously, the velocity represented by the function $F(G_\sigma * u_{\eta\eta}, G_\sigma * u_\eta)$ controls the position where the model develops shocks; however, it controls neither the intensity of the velocity according to the features of the signal (image) in different regions, nor what we target in the enhancement and restoration process. These issues motivated us to propose a model which takes them into account in Part I of this paper. The well-posedness of the obtained models within the framework of the generalized functions space was also proved.

2.2. The proposed model

In this subsection, we recall the one- and two-dimensional models proposed in Part I, as well as the interpretation of the models in the generalized functions algebra.

2.2.1. One-dimensional signal case

In Part I of this paper, we proposed the following quasi-linear hyperbolic equation with discontinuous coefficients as a generalized model for one-dimensional restoration and enhancement signals:

$$\begin{aligned} &u_t + a(x)F(u_{x^2}, u_x)\partial_x f\big(u(x)\big) = 0, \\ &u(x, 0) = u^0(x) \quad \text{in } \mathcal{G} \text{ and } (x, t) \in \mathbb{R} \times \mathbb{R}^+, \end{aligned} \tag{1}$$

where $\mathcal{G}$ is the generalized functions algebra, F is a regular function that controls the position where the model should create shocks, and the coefficients $a(x)$ (which is discontinuous) and f (a regular function) control the shock velocity according to the characteristics of the original signal and/or what is being targeted. For instance, these coefficients could focus processing on specific regions by setting the function equal to one for these areas and zero elsewhere (this is a specific case where $a(x)$ is a discontinuous function). With this coefficient, we can also simplify the model by setting the function F equal to one, and having a play the same role as F, but using the initial condition (signal). As a result, this function is only computed once, at the beginning of the process. Furthermore, we believe that by doing so, we avoid the problem of the edges' location, which can move during the process. In Section 3, we will demonstrate through tests how controlling the propagation speed (velocity) can make the restoration process appreciably faster. Lastly, the function f also allows the shocks' velocity to be controlled, according to the signal produced each time.

This equation is studied within the framework of the generalized functions theory by replacing the coefficients $a(\cdot)$ and the initial condition $u^0(\cdot)$ by the generalized functions, $A(\cdot)$ and $U^0(\cdot)$. These functions are obtained by a regularization of $a(\cdot)$ and $u^0(\cdot)$ (using mollifiers) and taking the class of equivalence, that is:

$$A = \operatorname{class}\big\{a^\varepsilon(\cdot),\ 0 < \varepsilon < 1\big\}, \qquad U^0 = \operatorname{class}\big\{u^{0,\varepsilon}(\cdot),\ 0 < \varepsilon < 1\big\},$$

where

$$a^\varepsilon = a * \left(\frac{1}{h_1(\varepsilon)}\rho\left(\frac{x}{h_1(\varepsilon)}\right)\right), \qquad u^{0,\varepsilon} = u^0 * \left(\frac{1}{h_2(\varepsilon)}\rho_1\left(\frac{x}{h_2(\varepsilon)}\right)\right).$$

ρ and ρ_1 are C^∞ smoothing functions (mollifiers) supported on the unit ball. The operator $*$ is the convolution product. The scale variables $h_1(\varepsilon)$ and $h_2(\varepsilon)$ are functions which tend conveniently to 0, and are chosen so that the previous function and their derivatives are moderate functions. To do so, choosing $h_i(\varepsilon) = (\log(1/\varepsilon))^{-1}$ is sufficient in order to have $\exp(h_1(\varepsilon)) = O(1/\varepsilon^N)$, for $N \in \mathbb{N}$.

The classical derivatives are also replaced by regularized derivatives. We have proved in Part I that the so-obtained equation admits a unique generalized solution referred to it by U. The representative u^ε of U satisfies the following equation (we set $h_1 = h_2 = h$). See Part I for details.

(a) If $a(\cdot)F(\cdot,\cdot)f'(\cdot) > 0$ then

$$\begin{aligned}\partial_t u^\varepsilon(x,t) &= -a^\varepsilon(x)F\begin{pmatrix}\frac{u^\varepsilon(x,t)-2u^\varepsilon(x-h,t)+u^\varepsilon(x-2h,t)}{h^2},\\ \frac{u^\varepsilon(x,t)-u^\varepsilon(x-h,t)}{h}\end{pmatrix}\\ &\quad\times f'\big(u^\varepsilon(x,t)\big)\left(\frac{u^\varepsilon(x,t)-u^\varepsilon(x-h,t)}{h}\right),\\ u^\varepsilon(x,0) &= u^{0,\varepsilon} \quad \text{(with } u^{0,\varepsilon} \text{ a } \mathcal{C}^\infty \text{ function and } u^0 = \text{class of } u^{0,\varepsilon}\text{).}\end{aligned} \tag{2}$$

(b) If $a(\cdot)F(\cdot,\cdot)f'(\cdot) < 0$ then

$$\begin{aligned}\partial_t u^\varepsilon(x,t) &= -a^\varepsilon(x)F\begin{pmatrix}\frac{u^\varepsilon(x+h,t)-2u^\varepsilon(x,t)+u^\varepsilon(x-h,t)}{h^2},\\ \frac{u^\varepsilon(x+h,t)-u^\varepsilon(x,t)}{h}\end{pmatrix}\\ &\quad\times f'\big(u^\varepsilon(x+h,t)\big)\left(\frac{u^\varepsilon(x+h,t)-u^\varepsilon(x,t)}{h}\right),\\ u^\varepsilon(x,0) &= u^{0,\varepsilon} \quad \text{(with } u^{0,\varepsilon} \text{ a } \mathcal{C}^\infty \text{ function and } u^0 = \text{class of } u^{0,\varepsilon}\text{).}\end{aligned} \tag{3}$$

(c) If $a(\cdot)F(\cdot,\cdot)f'(\cdot)$ has an unknown sign then

$$\begin{aligned}&\partial_t v^\varepsilon(y,\tau)\\ &\quad= -\frac{1}{h}\Big[\partial_{\lambda_3}\Im\big(y,\tau,\tfrac{v^\varepsilon(y,\tau)-2v^\varepsilon(y-h,\tau)+v^\varepsilon(y-2h,\tau)}{(h)^2},\tfrac{v^\varepsilon(y,\tau)-v^\varepsilon(y-h,\tau)}{h},v^\varepsilon(y,\tau)\big)\Big]\\ &\qquad\times\big(v^\varepsilon(y,\tau)-v^\varepsilon(y-h,\tau)\big),\\ &v^\varepsilon(y,0) = v^{0,\varepsilon} \quad \text{(with } v^{0,\varepsilon} \text{ a } \mathcal{C}^\infty \text{ function and } v^0 = \text{class of } v^{0,\varepsilon}\text{),}\end{aligned} \tag{4}$$

where

$$\begin{aligned}&y = x - ct \quad \text{and} \quad \tau = t,\\ &v^\varepsilon(y,\tau) = u^\varepsilon(x,t),\\ &c < \inf\big\{a^\varepsilon(x)F(\lambda_1\lambda_2)f'(\lambda_3),\ -M < \lambda_1,\ \lambda_2,\lambda_3 < M,\ x \in \mathbb{R},\ \varepsilon > 0\big\},\\ &\Im(y,\tau,\lambda_1,\lambda_2,\lambda_3) = a^\varepsilon(y+c\tau)F(\lambda_1,\lambda_2)f(\lambda_3) - c\lambda_3,\end{aligned}$$

$$a^{h_1(\varepsilon)} = a * \left(\frac{1}{h_1(\varepsilon)}\rho\left(\frac{x}{h_1(\varepsilon)}\right)\right), \qquad u^{0,h_3(\varepsilon)} = u^0 * \left(\frac{1}{h_2(\varepsilon)}\rho_1\left(\frac{x}{h_2(\varepsilon)}\right)\right).$$

(d) Viscous profile:

$$\begin{aligned}
\partial_t u^\varepsilon(x,t) &= -a^\varepsilon(x) F\left(\tfrac{u^\varepsilon(x,t)-2u^\varepsilon(x-h,t)+u^\varepsilon(x-2h,t)}{h^2}, \tfrac{u^\varepsilon(x,t)-u^\varepsilon(x-h,t)}{h}\right) \\
&\quad \times f'\big(u^\varepsilon(x,t)\big)\left(\frac{u^\varepsilon(x,t)-u^\varepsilon(x-h,t)}{h}\right) - c\frac{h}{2}\frac{\partial^2}{\partial x^2}u^\varepsilon(x-\theta h,t), \\
&\quad 0<\theta<1,\ \theta=\theta(x,t,h), \\
u^\varepsilon(x,0) &= u^{0,\varepsilon} \quad \text{(with } u^{0,\varepsilon} \text{ a } \mathcal{C}^\infty \text{ function and } u^0 = \text{class of } u^{0,\varepsilon}\text{).}
\end{aligned} \tag{5}$$

2.2.2. Two-dimensional signal case

For two-dimensional cases (images), we have proposed the following quasi-linear hyperbolic equation:

$$\begin{aligned}
&u_t + a_1 F_1(\Delta u, u_x)\partial_x f_1(u) + a_2 F_2(\Delta u, u_y)\partial_y f_2(u) = 0 \\
&\quad \text{in } \mathcal{G},\ (x,y,t) \in \mathbb{R}^2 \times \mathbb{R}^+,
\end{aligned} \tag{6}$$

where a_1, a_2, f_1, f_2, F_1 and F_2 are functions similar to the one-dimensional case. Same result of existence and uniqueness of generalized solution of Eq. (6) is proved. Furthermore, the representative u^ε of the generalized solution satisfies the following equation (refer to Part I for details).

(a) $a_1(\cdot)F_1(\cdot,\cdot)f_1'(\cdot) > 0$ and $a_2(\cdot)F_2(\cdot,\cdot)f_2'(\cdot) > 0$ case:

$$\begin{aligned}
\partial_t u^\varepsilon(x,t) &= -a_1^\varepsilon(x,y) F_1\left(\begin{array}{l}\frac{u^\varepsilon(x,y,t)-2u^\varepsilon(x-h_1,y,t)+u^\varepsilon(x-2h_1,y,t)}{h_1^2} \\ \quad + \frac{u^\varepsilon(x,y,t)-2u^\varepsilon(x,y-h_2,t)+u^\varepsilon(x_1,y-2h_2,t)}{h_2^2}, \\ \frac{u^\varepsilon(x,y,t)-u^\varepsilon(x-h_1,y,t)}{h_1}\end{array}\right) \\
&\quad \times f_1'\big(u^\varepsilon(x,y,t)\big)\left(\frac{u^\varepsilon(x,y,t)-u^\varepsilon(x-h_1,y,t)}{h_1}\right) \\
&\quad - a_2^\varepsilon(x,y) F_2\left(\begin{array}{l}\frac{u^\varepsilon(x,y,t)-2u^\varepsilon(x-h_1,y,t)+u^\varepsilon(x-2h_1,y,t)}{h_1^2} \\ \quad + \frac{u^\varepsilon(x,y,t)-2u^\varepsilon(x,y-h_2,t)+u^\varepsilon(x_1,y-2h_2,t)}{h_2^2}, \\ \frac{u^\varepsilon(x,y,t)-u^\varepsilon(x,y-h_2,t)}{h_2}\end{array}\right) \\
&\quad \times f_2'\big(u^\varepsilon(x,y,t)\big)\left(\frac{u^\varepsilon(x,y,t)-u^\varepsilon(x,y-h_2,t)}{h_2}\right), \\
u^\varepsilon(x,y,0) &= u^{0,\varepsilon} \quad \text{(with } u^{0,\varepsilon} \text{ a } C^\infty \text{ function and } u^0 = \text{class of } u^{0,\varepsilon}\text{).}
\end{aligned} \tag{7}$$

(b) $a_1(\cdot)F_1(\cdot,\cdot)f_1'(\cdot) < 0$ and $a_2(\cdot)F_2(\cdot,\cdot)f_2'(\cdot) < 0$ case:

$$\partial_t u^\varepsilon(x,t) = -a_1^\varepsilon(x,y) F_1\left(\begin{array}{l}\frac{u^\varepsilon(x+h_1,y,t)-2u^\varepsilon(x,y,t)+u^\varepsilon(x-h_1,y,t)}{h_1^2} \\ \quad + \frac{u^\varepsilon(x,y+h_2,t)-2u^\varepsilon(x,y,t)+u^\varepsilon(x_1,y-h_2,t)}{h_2^2}, \\ \frac{u^\varepsilon(x+h_1,y,t)-u^\varepsilon(x,y,t)}{h_1}\end{array}\right)$$

$$\times f_1'\big(u^\varepsilon(x,y,t)\big)\left(\frac{u^\varepsilon(x+h_1,y,t)-u^\varepsilon(x,y,t)}{h_1}\right)$$

$$-a_2^\varepsilon(x,y)F_2\left(\begin{array}{c}\frac{u^\varepsilon(x+h_1,y,t)-2u^\varepsilon(x,y,t)+u^\varepsilon(x-h_1,y,t)}{h_1^2}\\ +\frac{u^\varepsilon(x,y+h_2,t)-2u^\varepsilon(x,y,t)+u^\varepsilon(x_1,y-h_2,t)}{h_2^2},\\ \frac{u^\varepsilon(x,y+h_2,t)-u^\varepsilon(x,y,t)}{h_2}\end{array}\right)$$

$$\times f_2'\big(u^\varepsilon(x,y,t)\big)\left(\frac{u^\varepsilon(x,y+h_2,t)-u^\varepsilon(x,y,t)}{h_2}\right),$$

$$u^\varepsilon(x,y,0)=u^{0,\varepsilon}\quad(\text{with } u^{0,\varepsilon}\text{ a }\mathcal{C}^\infty\text{ function and } u^0=\text{class of } u^{0,\varepsilon}). \tag{8}$$

(c) Case of $a_1(\cdot)F_1(\cdot,\cdot)f_1'(\cdot)$ and $a_2(\cdot)F_2(\cdot,\cdot)f_2'(\cdot)$ with an unknown sign:

$$\partial_\tau v^\varepsilon(r,s,\tau)=-\frac{1}{h_1}\left[\partial_{\lambda_3}\Im_1\left(\begin{array}{c}r,s,\tau,\frac{v^\varepsilon(r,s,\tau)-2v^\varepsilon(r-h_1,s,\tau)+v^\varepsilon(r-2h_1,s,\tau)}{h_1^2}\\ +\frac{v^\varepsilon(r,s,\tau)-2v^\varepsilon(r,s-h_2,\tau)+v^\varepsilon(r,s-2h_2,\tau)}{h_2^2},\\ \frac{v^\varepsilon(r,s,\tau)-v^\varepsilon(r-h_1,s,\tau)}{h_1},v^\varepsilon(r,s,\tau)\end{array}\right)\right.$$

$$\left.\times\big(v^\varepsilon(r,s,\tau)-v^\varepsilon(r-h_1,s,\tau)\big)\right]$$

$$-\frac{1}{h_2}\left[\partial_{\lambda_3}\Im_2\left(\begin{array}{c}r,s,\tau,\frac{v^\varepsilon(r,s,\tau)-2v^\varepsilon(r-h_1,s,\tau)+v^\varepsilon(r-2h_1,s,\tau)}{h_1^2}\\ +\frac{v^\varepsilon(r,s,\tau)-2v^\varepsilon(r,s-h_2,\tau)+v^\varepsilon(r,s-2h_2,\tau)}{h_2^2},\\ \frac{v^\varepsilon(r,s,\tau)-v^\varepsilon(r,s-h_2,\tau)}{h_2},v^\varepsilon(r,s,\tau)\end{array}\right)\right.$$

$$\left.\times\big(v^\varepsilon(r,s,\tau)-v^\varepsilon(r,s-h_2,\tau)\big)\right],$$

$$v^\varepsilon(r,s,0)=u^{0,\varepsilon}\quad(\text{with } u^{0,\varepsilon}\text{ a }\mathcal{C}^\infty\text{ function and } u^0=\text{class of } u^{0,\varepsilon}), \tag{9}$$

where

$$\Im_1(r,s,\tau,\lambda_1,\lambda_2,\lambda_3)=a_1^\varepsilon(r+c_1\tau,s+c_2\tau)F_1(\lambda_1,\lambda_2)f_1(\lambda_3)-c\lambda_3,$$

$$\Im_2(r,s,\tau,\lambda_1,\lambda_2,\lambda_3)=a_2^\varepsilon(r+c_1\tau,s+c_2\tau)F_2(\lambda_1,\lambda_2)f_2(\lambda_3)-c\lambda_3,$$

$$c_1<\inf_{\substack{-M<\lambda_1<M,\ -M<\lambda_2<M\\ -M<\lambda_3<M\\ x,y\in\Re,\ \varepsilon>0}}\big\{a_1^\varepsilon(x,y)F_1(\lambda_1\lambda_2)f_1'(\lambda_3)\big\},$$

$$c_2<\inf_{\substack{-M<\lambda_1<M,\ -M<\lambda_2<M\\ -M<\lambda_3<M\\ x,y\in\Re,\ \varepsilon>0}}\big\{a_2^\varepsilon(x,y)F_2(\lambda_1\lambda_2)f_2'(\lambda_3)\big\}.$$

(d) Viscous profile:

$$\begin{aligned}
\partial_t u^\varepsilon(x,t) = {} & -a_1^\varepsilon(x,y) F_1 \begin{pmatrix} \frac{u^\varepsilon(x,y,t)-2u^\varepsilon(x-h_1,y,t)+u^\varepsilon(x-2h_1,y,t)}{h_1^2} \\ \quad + \frac{u^\varepsilon(x,y,t)-2u^\varepsilon(x,y-h_2,t)+u^\varepsilon(x_1,y-2h_2,t)}{h_2^2}, \\ \frac{u^\varepsilon(x,y,t)-u^\varepsilon(x-h_1,y,t)}{h_1} \end{pmatrix} \\
& \times f_1'\big(u^\varepsilon(x,y,t)\big)\left(\frac{u^\varepsilon(x,y,t)-u^\varepsilon(x-h_1,y,t)}{h_1}\right) \\
& - c_1 \frac{h_1}{2}\frac{\partial^2}{\partial x^2} u^\varepsilon(x-\theta_1 h_1, y, t) \quad \big(0<\theta_1<1,\ \theta_1=\theta_1(x,y,t,h_1)\big) \\
& - a_2^\varepsilon(x,y) F_2 \begin{pmatrix} \frac{u^\varepsilon(x,y,t)-2u^\varepsilon(x-h_1,y,t)+u^\varepsilon(x-2h_1,y,t)}{h_1^2} \\ \quad + \frac{u^\varepsilon(x,y,t)-2u^\varepsilon(x,y-h_2,t)+u^\varepsilon(x_1,y-2h_2,t)}{h_2^2}, \\ \frac{u^\varepsilon(x,y,t)-u^\varepsilon(x,y-h_2,t)}{h_2} \end{pmatrix} \\
& \times f_2'\big(u^\varepsilon(x,y,t)\big)\left(\frac{u^\varepsilon(x,y,t)-u^\varepsilon(x,y-h_2,t)}{h_2}\right) \\
& - c_2 \frac{h_2}{2}\frac{\partial^2}{\partial y^2} u^\varepsilon(x, y-\theta_2 h_2, t) \quad \big(0<\theta_2<1,\ \theta_2=\theta_2(x,y,t,h_2)\big).
\end{aligned} \tag{10}$$

3. Numerical scheme for one-dimensional signal restoration and enhancement

Since the function θ in (5) is unknown, we derive the numerical scheme from (2) and (3) according to the local sign of the propagation velocity. We then propose the numerical scheme below.

Let us first set the following classical notations: $u_i^{\varepsilon,n} = u^\varepsilon(x_i = i\,\Delta x, t_n = n\Delta t)$, Δx and Δt are the spatial and time meshsizes, respectively. We then make the classical approximation

$$\partial_t u^\varepsilon(t_n, x_i) = \frac{u_i^{\varepsilon,n+1} - u_i^{\varepsilon,n}}{\Delta t}.$$

For each ordered pair (x_i, t_n), the approximation $u_i^{\varepsilon,n}$ of $u^\varepsilon(x_i,t_n)$ is the discrete solution of (2) if $a(x_x)F(\Delta u(x_i,t_n))f'(u^\varepsilon(x_i,t_n)) > 0$, and the discrete solution of (3) if $a(x_x)F(\Delta u(x_i,t_n))f'(u^\varepsilon(x_i,t_n)) < 0$. This leads to the following numerical scheme (we set $h = \Delta x$ and $r = \Delta x/\Delta t$).

$$\begin{aligned}
u_i^{\varepsilon,n+1} = {} & u_i^n - r\max\Big[0, a_i F\Big(\tfrac{u_{i+1}^{\varepsilon,n}-2u_i^{\varepsilon,n}+u_{i-1}^{\varepsilon,n}}{h^2}, \tfrac{u_i^{\varepsilon,n}-u_{i-1}^{\varepsilon,n}}{h}\Big) f'\big(u_i^{\varepsilon,n}\big)\Big]\big(u_i^{\varepsilon,n} - u_{i-1}^{\varepsilon,n}\big) \\
& - r\min\Big[0, a_i F\Big(\tfrac{u_{i+1}^{\varepsilon,n}-2u_i^{\varepsilon,n}+u_{i-1}^{\varepsilon,n}}{h^2}, \tfrac{u_{i+1}^{\varepsilon,n}-u_i^{\varepsilon,n}}{h}\Big) f'\big(u_i^{\varepsilon,n}\big)\Big]\big(u_{i+1}^{\varepsilon,n} - u_i^{\varepsilon,n}\big), \\
u_i^{\varepsilon,0} = {} & u^{\varepsilon,0}(ih).
\end{aligned} \tag{11}$$

3.1. Stability results

Let us now give a stability proposition for numerical scheme (11).

Proposition 3.1.1. *Assume that a belong in $BV(\mathbb{R}) \cap L^\infty(\mathbb{R})$, F and f are regular functions. Under the CFL (Courant–Friedrichs–Lewy) condition* [5], *$r|aFf'| < 1/2$, the above scheme is stable for the L^∞-norm, for the total variation in space, as well as for the total variation in time in the Tonnelli–Cesari sense, that is*:

$$\text{(i)} \quad \left|u_i^{\varepsilon,n}\right| \leqslant \|u_0\|_{L^\infty(\Re)}, \quad \forall i \in Z,\ \forall n \in \mathbb{N},$$

$$\text{(ii)} \quad \sum_{i\in Z} \left|u_{i+1}^{\varepsilon,n} - u_i^{\varepsilon,n}\right| \leqslant TV(u_0), \quad \forall n \in \mathbb{N},$$

$$\text{(iii)} \quad \sum_{i\in Z} \left|u_i^{\varepsilon,n+1} - u_i^{\varepsilon,n}\right| \leqslant TV(u_0), \quad \forall n \in \mathbb{N}.$$

Proof. First set

$$\alpha_i^n = \max\Big[0, a_i F\Big(\tfrac{u_{i+1}^{\varepsilon,n} - 2u_i^{\varepsilon,n} + u_{i-1}^{\varepsilon,n}}{h^2}, \tfrac{u_i^{\varepsilon,n} - u_{i-1}^{\varepsilon,n}}{h}\Big) f'\big(u_i^{\varepsilon,n}\big)\Big]$$

and

$$\beta_i = \min\Big[0, a_i F\Big(\tfrac{u_{i+1}^{\varepsilon,n} - 2u_i^{\varepsilon,n} + u_{i-1}^{\varepsilon,n}}{h^2}, \tfrac{u_{i+1}^{\varepsilon,n} - u_i^{\varepsilon,n}}{h}\Big) f'\big(u_i^{\varepsilon,n}\big)\Big].$$

The numerical scheme is then rewritten as follows:

$$u_i^{\varepsilon,n+1} = u_i^n - r\alpha_i^n\big(u_i^{\varepsilon,n} - u_{i-1}^{\varepsilon,n}\big) - r\beta_i^n\big(u_{i+1}^{\varepsilon,n} - u_i^{\varepsilon,n}\big). \tag{12}$$

Using the CFL condition, $\|raFf'\| < 1/2$, we have

$$\alpha_i^n \geqslant 0 \quad \text{and} \quad \left|r\alpha_i^n\right| \leqslant \frac{1}{2}, \tag{13}$$

$$\beta_i^n \leqslant 0 \quad \text{and} \quad \left|r\beta_i^n\right| \leqslant \frac{1}{2}. \tag{14}$$

Proof of (i). From (12) we have

$$u_i^{\varepsilon,n+1} = \big(1 - \alpha_i^n + r\beta_i^n\big)u_i^n + r\alpha_i^n u_{i-1}^{\varepsilon,n} - r\beta_i^n u_{i+1}^{\varepsilon,n}.$$

Taking (13) and (14) into account, we achieve

$$\begin{aligned}\left|u_i^{\varepsilon,n+1}\right| &\leqslant \big(1 - r\alpha_i^n + r\beta_i^n\big)\left|u_i^n\right| + r\alpha_i^n\left|u_{i-1}^{\varepsilon,n}\right| - r\beta_i^n\left|u_{i+1}^{\varepsilon,n}\right| \\ &\leqslant \big(1 - r\alpha_i^n + r\beta_i^n\big)\sup_{i\in\mathbb{Z}}\left|u_i^{\varepsilon,n}\right| + r\alpha_i^n \sup_{i\in\mathbb{Z}}\left|u_{i-1}^{\varepsilon,n}\right| - r\beta_i^n \sup_{i\in\mathbb{Z}}\left|u_{i+1}^{\varepsilon,n}\right| = \sup_{i\in\mathbb{Z}}\left|u_i^{\varepsilon,n}\right|.\end{aligned}$$

Then, recursively, we obtain

$$\left|u_i^{\varepsilon,n+1}\right| \leqslant \sup_i u_i^{\varepsilon,0} \leqslant \|u_0\|_{L^\infty(\Re)}.$$

To prove (ii) and (iii), we first need to prove the following two assertions:

$$(*)\quad \sum_{i\in Z}\left|u_i^{n+1}-u_i^n\right|\leqslant\sum_{i\in Z}\left|u_{i+1}^n-u_i^n\right|,$$

$$(**)\quad \sum_{i\in Z}\left|u_{i+1}^{n+1}-u_i^{n+1}\right|\leqslant\sum_{i\in Z}\left|u_{i+1}^n-u_i^n\right|.$$

As such, (ii) is obtained recursively from $(**)$, and (iii) is obtained by combining $(*)$ and $(**)$ in a recursive fashion.

Proof of $(*)$. From (12), we have the inequality

$$\left|u_i^{\varepsilon,n+1}-u_i^{\varepsilon,n}\right|\leqslant\alpha_i^n r\left|u_i^{\varepsilon,n}-u_{i-1}^{\varepsilon,n}\right|+r\left|\beta_i^n\right|\left|u_{i+1}^{\varepsilon,n}-u_i^{\varepsilon,n}\right|.$$

Using (13) and (14) once again, we obtain

$$\left|u_i^{\varepsilon,n+1}-u_i^{\varepsilon,n}\right|\leqslant\frac{1}{2}\left|u_i^{\varepsilon,n}-u_{i-1}^{\varepsilon,n}\right|+\frac{1}{2}\left|u_{i+1}^{\varepsilon,n}-u_i^{\varepsilon,n}\right|.$$

The two quantities on the right are the same up to a shift of index i. By summing over the index i we obtain $(*)$, specifically

$$\sum_{i\in\mathbb{Z}}\left|u_i^{\varepsilon,n+1}-u_i^{\varepsilon,n}\right|\leqslant\sum_{i\in\mathbb{Z}}\left|u_{i+1}^{\varepsilon,n}-u_i^{\varepsilon,n}\right|.$$

Proof of $(**)$. Let us express (12) at i and $i+1$:

$$u_i^{\varepsilon,n+1}=u_i^n-r\alpha_i^n\left(u_i^{\varepsilon,n}-u_{i-1}^{\varepsilon,n}\right)-r\beta_i^n\left(u_{i+1}^{\varepsilon,n}-u_i^{\varepsilon,n}\right),$$
$$u_{i+1}^{\varepsilon,n+1}=u_{i+1}^n-r\alpha_{i+1}^n\left(u_{i+1}^{\varepsilon,n}-u_i^{\varepsilon,n}\right)-r\beta_{i+1}^n\left(u_{i+2}^{\varepsilon,n}-u_{i+1}^{\varepsilon,n}\right).$$

We have

$$u_{i+1}^{n+1}-u_i^{n+1}=\left(1+r\beta_1^n-r\alpha_{i+1}^n\right)\left(u_{i+1}^n-u_i^n\right)+r\alpha_i^n\left(u_i^n-u_{i-1}^n\right)-r\beta_{i+1}^n\left(u_{i+2}^n-u_{i+1}^n\right).$$

Taking (13) and (14) into account, we obtain

$$\left|u_{i+1}^{n+1}-u_i^{n+1}\right|\leqslant\left(1+r\beta_i^n-r\alpha_{i+1}^n\right)\left|u_{i+1}^n-u_i^n\right|+r\alpha_i^n\left|u_i^n-u_{i-1}^n\right|-r\beta_{i+1}^n\left|u_{i+2}^n-u_{i+1}^n\right|.$$

Summing over index i,

$$\sum_{i\in Z}\left|u_{i+1}^{n+1}-u_i^{n+1}\right|\leqslant\sum_{i\in Z}\left(1+r\beta_i^n-r\alpha_{i+1}^n\right)\left|u_{i+1}^n-u_i^n\right|+\sum_{i\in Z}r\alpha_i^n\left|u_i^n-u_{i-1}^n\right|-\sum_{i\in Z}r\beta_{i+1}^n\left|u_{i+2}^n-u_{i+1}^n\right|.$$

By shifting the index i forward and back in the last two quantities, we achieve

$$\sum_{i\in Z}\left|u_{i+1}^{n+1}-u_i^{n+1}\right|\leqslant\sum_{i\in Z}\left(1+r\beta_i^n-r\alpha_{i+1}^n\right)\left|u_{i+1}^n-u_i^n\right|+\sum_{i\in Z}r\alpha_{i+1}^n\left|u_{i+1}^n-u_i^n\right|-\sum_{i\in Z}r\beta_i^n\left|u_{i+1}^n-u_i^n\right|,$$

which finally gives us

$$\sum_{i\in Z}\left|u_{i+1}^{n+1}-u_i^{n+1}\right|\leqslant\sum_{i\in Z}\left|u_{i+1}^{n}-u_i^{n}\right|. \qquad \square$$

3.2. On a convergence of the numerical scheme

Let us now show a convergence result for the numerical solution of scheme (11) and demonstrate how the limit may be considered as a solution of Eq. (1). Also let us assume the condition on F as in [1,2,10], which is

$$rsF(r,s)\geqslant 0.$$

This condition prevents the quantities defined by the max and min in the numerical scheme from vanishing simultaneously for certain points.

From the maximum principle proved in Part I for the representatives, the sequence u^ε admits a subsequence (u^ε) that converges to u for the $\sigma(L^\infty, L^1)$ topology. u is said to be the macroscopic aspect to the generalized solution U given by the class of the sequence $(u^\varepsilon)_\varepsilon$ (see Part I for details). Now, we denote by u_h the function which is equal to u_i^n on the rectangle

$$I_i\times\left[\left(n-\frac{1}{2}\right)\Delta t,\left(n+\frac{1}{2}\right)\Delta t\right[\quad \text{where } I_i=[x_{i-1/2},x_{i+1/2}[\,.$$

Through the scheme's stability for the L^∞ norm, the function sequence u_h also admits a subsequence (u_h) that converges to $\bar{u}$ for the $\sigma(L^\infty([0,T[\times\mathbb{R}), L^1([0,T[\times\mathbb{R}))$ topology. After arranging that the subsequence indices are the same (we still refer to them as u^ε and u_h), we will now prove that $\bar{u}=u$. The convergence must be taken in the sense that the scheme converges to the macroscopic aspect of the generalized solution. From Eq. (2), to prove that (u_h) and (u^ε) have the same limit it is sufficient to prove that

$$\int_0^T\int_{\Re} a^\varepsilon(x)F\left(\begin{array}{c}\frac{u^\varepsilon(x,t)-2u^\varepsilon(x-h,t)+u^\varepsilon(x-2h,t)}{h^2},\\ \frac{u^\varepsilon(x,t)-u^\varepsilon(x-h,t)}{h}\end{array}\right)$$
$$\times\ f'\big(u^\varepsilon(x,t)\big)\big(u^\varepsilon(x,t)-u^\varepsilon(x-h,t)\big)\,dx\,dt\underset{h\to 0}{\to}0.$$

Let us begin by proving the following lemma.

Lemma 3.2.1. *The solution u^ε of* (2) *satisfies the following inequality*:

$$\frac{1}{h}\int_{\Re}\left|u^\varepsilon(x,t)-u^\varepsilon(x-h,t)\right|dx\leqslant\frac{1}{h}\int_{\Re}\left|u^{\varepsilon,0}(x)-u^{\varepsilon,0}(x-h)\right|dx\leqslant TV(u^0).$$

To prove this lemma, let us write (2) at x and $x-h$. Now let us take the difference and multiply by $\operatorname{sign}(u^\varepsilon(x,t)-u^\varepsilon(x-h,t))$ to obtain

$$
\begin{aligned}
&\partial_t \left|u^\varepsilon(x,t) - u^\varepsilon(x-h,t)\right| \\
&\quad = -a^\varepsilon(x) F\begin{pmatrix} \frac{u^\varepsilon(x,t)-2u^\varepsilon(x-h,t)+u^\varepsilon(x-2h,t)}{h^2}, \\ \frac{u^\varepsilon(x,t)-u^\varepsilon(x-h,t)}{h} \end{pmatrix} \\
&\qquad \times f'\big(u^\varepsilon(x,t)\big)\left|\frac{u^\varepsilon(x,t) - u^\varepsilon(x-h,t)}{h}\right| \\
&\qquad + a^\varepsilon(x-h) F\begin{pmatrix} \frac{u^\varepsilon(x-h,t)-2u^\varepsilon(x-2h,t)+u^\varepsilon(x-3h,t)}{h^2}, \\ \frac{u^\varepsilon(x-h,t)-u^\varepsilon(x-2h,t)}{h} \end{pmatrix} \\
&\qquad \times f'\big(u^\varepsilon(x-h,t)\big)\left(\frac{u^\varepsilon(x-h,t) - u^\varepsilon(x-2h,t)}{h}\right) \\
&\qquad \times \operatorname{sign}\big(u^\varepsilon(x,t) - u^\varepsilon(x-h,t)\big) \\
&\quad \leqslant -a^\varepsilon(x) F\begin{pmatrix} \frac{u^\varepsilon(x,t)-2u^\varepsilon(x-h,t)+u^\varepsilon(x-2h,t)}{h^2}, \\ \frac{u^\varepsilon(x,t)-u^\varepsilon(x-h,t)}{h} \end{pmatrix} \\
&\qquad \times f'\big(u^\varepsilon(x,t)\big)\left|\frac{u^\varepsilon(x,t) - u^\varepsilon(x-h,t)}{h}\right| \\
&\qquad + a^\varepsilon(x-h) F\begin{pmatrix} \frac{u^\varepsilon(x-h,t)-2u^\varepsilon(x-2h,t)+u^\varepsilon(x-3h,t)}{h^2}, \\ \frac{u^\varepsilon(x-h,t)-u^\varepsilon(x-2h,t)}{h} \end{pmatrix} \\
&\qquad \times f'\big(u^\varepsilon(x-h,t)\big)\left|\frac{u^\varepsilon(x-h,t) - u^\varepsilon(x-2h,t)}{h}\right|.
\end{aligned}
$$

Therefore,

$$
\int_{\Re} \partial_t \left|u^\varepsilon(x,t) - u^\varepsilon(x-h,t)\right| dx \leqslant 0,
$$

the integration from 0 to t yields the result.

From this lemma and the boundedness condition taken on a and F, we obtain

$$
\begin{aligned}
&\int_0^T\!\!\int_{\Re} a^\varepsilon(x) F^\varepsilon\begin{pmatrix} \frac{u^\varepsilon(x,t)-2u^\varepsilon(x-h,t)+u^\varepsilon(x-2h,t)}{h^2}, \\ \frac{u^\varepsilon(x,t)-u^\varepsilon(x-h,t)}{h} \end{pmatrix} \\
&\qquad \times\ f'\big(u^\varepsilon(x,t)\big)\big(u^\varepsilon(x,t) - u^\varepsilon(x-h,t)\big)\,dx\,dt \\
&\quad \leqslant c\int_0^T\!\!\int_{\Re} \left|u^\varepsilon(x,t) - u^\varepsilon(x-h,t)\right| dx\,dt \leqslant ch\int_0^T\!\!\int_{\Re} \left|\frac{u^\varepsilon(x,t) - u^\varepsilon(x-h,t)}{h}\right| dx\,dt \\
&\quad \leqslant hTcTV(u^0),
\end{aligned}
$$

which achieves the convergence result.

We now return to the case where $a(\cdot)F(\cdot,\cdot)f'(\cdot)$ has an unknown sign. The corresponding numerical scheme could be derived by expressing (4) with the initial variables, x and t (see Part I). We then obtain

$$v^\varepsilon(y,\tau) = u^\varepsilon(x,t) = u^\varepsilon(y + c\tau, \tau)$$

and

$$\begin{aligned}
&\partial_t u^\varepsilon(x,t) + c\partial_x u^\varepsilon(x,t) \\
&\quad = -\left[a^\varepsilon(x)F^\varepsilon\left(\tfrac{u^\varepsilon(x,t)-2u^\varepsilon(x-h,t)+u^\varepsilon(x-2h,t)}{h^2}, \tfrac{u^\varepsilon(x,t)-u^\varepsilon(x-h,t)}{h}\right)f'\left(u^\varepsilon(x,t)\right) - c\right] \\
&\qquad \times \left(\frac{u^\varepsilon(x,t) - u^\varepsilon(x-h,t)}{h}\right).
\end{aligned}$$

This equation is of the type

$$u_t + c\partial_x u(x) = G(u),$$

with a non-positive characteristic slope c. Thus, we proceed as in the case of the non-positive shock velocity, and then, the regularized derivative $\bar{\partial}_x u(x)$ for a given representative is computed as in (3). Then, u^ε satisfies the following equation:

$$\begin{aligned}
\partial_t u^\varepsilon(x,t) = -&\left[a^\varepsilon(x)F^\varepsilon\left(\begin{matrix}\frac{u^\varepsilon(x,t)-2u^\varepsilon(x-h,t)+u^\varepsilon(x-2h,t)}{h^2}, \\ \frac{u^\varepsilon(x,t)-u^\varepsilon(x-h,t)}{h}\end{matrix}\right)f'\left(u^\varepsilon(x,t)\right) - c\right] \\
&\times \left(\frac{u^\varepsilon(x,t) - u^\varepsilon(x-h,t)}{h}\right) - c\left(\frac{u^\varepsilon(x+h,t) - u^\varepsilon(x,t)}{h}\right).
\end{aligned}$$

Note that the regularized derivatives are obtained by a convolution with a mollifier supported in $[-h,h]$. Hence, we choose c such that

$$c = \min\left[0, \inf_{\substack{-h\leqslant x\leqslant h \\ t_n\leqslant t\leqslant t_{n+1}}}\left[a(x)F\left(u^\varepsilon_{xx}(x,t), u^\varepsilon_x(x,t)\right)f'\left(u^\varepsilon(x,t)\right)\right]\right]$$

on each $[-h,h]$. Then replace in the above equation on points (x_i,t_n) and make the approximation

$$\begin{aligned}
&\inf_{\substack{-h+x_i\leqslant x\leqslant h+x_i \\ t_n\leqslant t\leqslant t_{n+1}}}\left[a(x)F\left(u^\varepsilon_{xx}(x,t), u^\varepsilon_x(x,t)\right)f'\left(u^\varepsilon(x,t)\right)\right] \\
&\quad \approx a^\varepsilon(x_i)F\left(\begin{matrix}\frac{u^\varepsilon(x_i,t_n)-2u^\varepsilon(x_i-h,t_n)+u^\varepsilon(x_i-2h,t_n)}{h^2}, \\ \frac{u^\varepsilon(x_i,t_n)-u^\varepsilon(x_i-h,t_n)}{h}\end{matrix}\right)f'\left(u^\varepsilon(x_i,t_n)\right).
\end{aligned}$$

We achieve numerical scheme (11) and the above proof is applied. □

3.3. Tests and discussion

We tested the model in three experiments using the explicit proposed numerical scheme to enhance and restore signals. In the first experiment, we tested the ability of the model to remove noise and create discontinuities (shocks). We also compared the results obtained

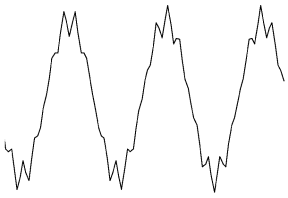

Noisy sinusoidal function

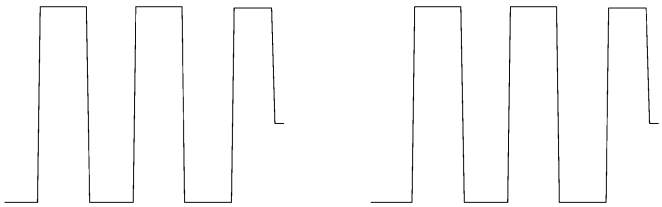

(a) Restoration using edge detection for each signal produced.

(b) Restoration using edge detection for the original signal only.

Fig. 1. We can see that the same results are obtained whether edge detection is used for each signal produced or only for the original signal. Processing time can consequently be shortened.

by considering the edge detection for each generated signal according to time with the results obtained by considering the edge detection for the original signal only. In the second experiment, we tested the model's ability to restore noisier signals, and we finished in the third experiment by testing the influence of the coefficients introduced in the model (velocity control) on the results. In all of these experiments, we used a kernel with compact support (KCS) from [9] (with ε as the scale parameter) as a mollifier to smooth the original signal (and obtain $u^{\varepsilon,0}$). These kernels are a family of mollifiers according to the definition given in Part I.

In Fig. 1, we apply the numerical scheme to a noisy sinusoidal signal with the following parameters: $h(\varepsilon) = 5$, $r = 0.45$, and $f(u) = u$. For the case on the left, we set $F(u, v) = \operatorname{sign}(u)\operatorname{sign}(v)$ (here the function sign is regularized to obtain a C^∞ function. Another type of function-like sigmoid can be used to achieve this task) and $a \equiv 1$. For the case on the right, we set $F(u, v) \equiv 1$ and $a \equiv \operatorname{sign}(\Delta u^0)\operatorname{sign}(u_x^0)$ as a generalized functions (which means that we consider a representative $a^\varepsilon \equiv \operatorname{sign}(\Delta u^{\varepsilon,0})\operatorname{sign}(u_x^{\varepsilon,0})$ of the generalized functions; $\Delta u^{\varepsilon,0}$, $u_x^{\varepsilon,0}$ are computed in a manner similar to Δu^ε, u_x^ε using regularized derivatives with mollifiers chosen from Eqs. (2), (3), etc.). a^ε plays the role of detecting edges and determining the enhancement direction. This operation is performed on the original signal; as a result, the function is computed only once, at the beginning of the process. Furthermore, we believe that by doing so, we avoid the issue of the edges' location, which can move during the process. The results in both cases indicate that the noise is removed and the signal perfectly deconvoluted after 10 iterations. Consequently, the latter was adopted for all our tests. In Fig. 2, a gate signal is smoothed and sinusoidal noise

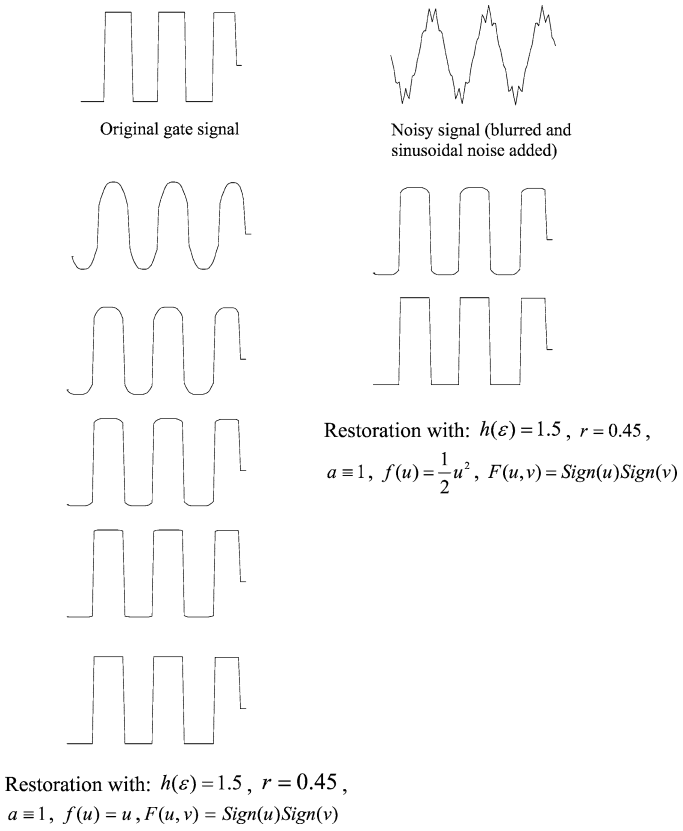

Fig. 2. Enhancement and restoration of a noisy gate signal, with different values of the speed control function f. The restored signals are displayed every second iteration for both experiments. We can see that the signal is perfectly restored for both choices. The same results obtained after five steps with less speed control $(f(u)=u)$ are obtained after only two steps when the speed control is heightened $(f(u)=(1/2)u^2)$.

was added. With the parameters $r=0.45$, $h(\varepsilon)=5$, $a\equiv \operatorname{sign}(\Delta u^0)\operatorname{sign}(u_x^0)$, $f(u)=u$ and $F(u,v)\equiv 1$, the signal is restored after 10 iterations, when the choice of $f(u)=(1/2)u^2$ (as in the Burger equation [5]) achieves the same results after only four iterations. Based on this test, we can appreciate the model's ability to restore very noisy signals, as well as the impact of controlling the velocity on the time process. The choice of $f(u)=(1/2)u^2$ favors the creation of discontinuities (shocks) near regions where the value of the function approaches ± 1, which makes the process faster than when using $f(u)=u$.

4. Numerical scheme for two-dimensional signal restoration and enhancement

We built our numerical scheme from the general case (the slope's sign is unknown). If we return to the initial variables x, y and t in (9) (see Part I for details), we obtain

$$v^\varepsilon(r,s,\tau)=u^\varepsilon(x,y,t)=u^\varepsilon(r+c_1\tau,s+c_2\tau,\tau)$$

and

$$\partial_\tau v^\varepsilon(r,s,\tau) = c_1\partial_x u^\varepsilon(x,y,t) + c_2\partial_y u^\varepsilon(x,y,t) + \partial_t u^\varepsilon(x,y,t),$$

$$\partial_t u^\varepsilon(x,t) + c_1\partial_x u^\varepsilon(x,t) + c_2\partial_y u^\varepsilon(x,t)$$

$$= -\left[a_1^\varepsilon(x,y) F_1 \begin{pmatrix} \frac{u^\varepsilon(x,y,t)-2u^\varepsilon(x-h_1,y,t)+u^\varepsilon(x-2h_1,y,t)}{h_1^2} \\ \quad + \frac{u^\varepsilon(x,y,t)-2u^\varepsilon(x,y-h_2,t)+u^\varepsilon(x_1,y-2h_2,t)}{h_2^2}, \\ \frac{u^\varepsilon(x,y,t)-u^\varepsilon(x-h_1,y,t)}{h_1} \end{pmatrix} \right.$$

$$\left. \times f_1'\big(u^\varepsilon(x,y,t)\big) - c_1 \left(\frac{u^\varepsilon(x,y,t) - u^\varepsilon(x-h_1,y,t)}{h_1} \right) \right]$$

$$- \left[a_2^\varepsilon(x,y) F_2 \begin{pmatrix} \frac{u^\varepsilon(x,y,t)-2u^\varepsilon(x-h_1,y,t)+u^\varepsilon(x-2h_1,y,t)}{h_1^2} \\ \quad + \frac{u^\varepsilon(x,y,t)-2u^\varepsilon(x,y-h_2,t)+u^\varepsilon(x_1,y-2h_2,t)}{h_2^2}, \\ \frac{u^\varepsilon(x,y,t)-u^\varepsilon(x,y-h_2,t)}{h_2} \end{pmatrix} \right.$$

$$\left. \times f_2'\big(u^\varepsilon(x,y,t)\big) - c_2 \left(\frac{u^\varepsilon(x,y,t) - u^\varepsilon(x,y-h_2,t)}{h_2} \right), \right]$$

$$u^\varepsilon(x,y,0) = u^{0,\varepsilon} \quad \text{(with } u^{0,\varepsilon} \text{ a } \mathcal{C}^\infty \text{ function and } u^0 = \text{class of } u^{0,\varepsilon}\text{)}.$$

This equation is of the type

$$\partial_t u^\varepsilon(x,t) + c_1\partial_x u^\varepsilon(x,t) + c_2\partial_y u^\varepsilon(x,t) = H(u).$$

Since the constants c_1 and c_2 are non-positive, we proceed as in the case of non-positive shock velocities (7). Then u^ε satisfies the following equation:

$$\partial_t u^\varepsilon(x,t) = -\left[a_1^\varepsilon(x,y) F_1 \begin{pmatrix} \frac{u^\varepsilon(x,y,t)-2u^\varepsilon(x-h_1,y,t)+u^\varepsilon(x-2h_1,y,t)}{h_1^2} \\ \quad + \frac{u^\varepsilon(x,y,t)-2u^\varepsilon(x,y-h_2,t)+u^\varepsilon(x_1,y-2h_2,t)}{h_2^2}, \\ \frac{u^\varepsilon(x,y,t)-u^\varepsilon(x-h_1,y,t)}{h_1} \end{pmatrix} \right.$$

$$\left. \times f_1'\big(u^\varepsilon(x,y,t)\big) - c_1 \left(\frac{u^\varepsilon(x,y,t) - u^\varepsilon(x-h_1,y,t)}{h_1} \right) \right]$$

$$- c_1 \left(\frac{u^\varepsilon(x+h_1,y,t) - u^\varepsilon(x,y,t)}{h_1} \right)$$

$$
- \left[a_2^{\varepsilon}(x,y) F_2 \left(\begin{array}{l} \frac{u^{\varepsilon}(x,y,t)-2u^{\varepsilon}(x-h_1,y,t)+u^{\varepsilon}(x-2h_1,y,t)}{h_1^2} \\ \quad + \frac{u^{\varepsilon}(x,y,t)-2u^{\varepsilon}(x,y-h_2,t)+u^{\varepsilon}(x_1,y-2h_2,t)}{h_2^2}, \\ \frac{u^{\varepsilon}(x,y,t)-u^{\varepsilon}(x,y-h_2,t)}{h_2} \end{array} \right) \right.
$$

$$
\left. \times f_2'\big(u^{\varepsilon}(x,y,t)\big) - c_2 \right] \left(\frac{u^{\varepsilon}(x,y,t) - u^{\varepsilon}(x,y-h_2,t)}{h_2} \right)
$$

$$
- c_2 \left(\frac{u^{\varepsilon}(x,y+h_2,t) - u^{\varepsilon}(x,y,t)}{h_2} \right).
$$

Using the same considerations as in the one-dimensional case for constants c_1 and c_2, and the approximation $u_{i,j}^{\varepsilon,n}$ of u^{ε} (a representative of u) at the point $(x_i, y_j, n\Delta t)$, where $x_i = i\Delta x$ and $x_j = j\Delta y$, and by setting $h_1 = \Delta x$, $h_2 = \Delta y$, $r_1 = \Delta x/\Delta t$, and $r_2 = \Delta y/\Delta t$, we achieve the following numerical scheme:

$$
u_{i,j}^{\varepsilon,n+1} = u_{i,j}^{\varepsilon,n} - r_1 \max \left[0, a_{i,j}^1 F_1 \left(\begin{array}{l} \frac{u_{i+1,j}^{\varepsilon,n}-2u_{i,j}^{\varepsilon,n}+u_{i-1,j}^{\varepsilon,n}}{h_1^2} + \frac{u_{i,j+1}^{\varepsilon,n}-2u_{i,j}^{\varepsilon,n}+u_{i,j-1}^{\varepsilon,n}}{h_1^2}, \\ \frac{u_{i,j}^{\varepsilon,n}-u_{i-1,j}^{\varepsilon,n}}{h_1} \end{array} \right) \right.
$$

$$
\left. \times f'\big(u_{i,j}^{\varepsilon,n}\big) \right] \big(u_{i,j}^{\varepsilon,n} - u_{i-1,j}^{\varepsilon,n}\big)
$$

$$
- r_1 \min \left[0, a_{i,j}^1 F_1 \left(\begin{array}{l} \frac{u_{i+1,j}^{\varepsilon,n}-2u_{i,j}^{\varepsilon,n}+u_{i-1,j}^{\varepsilon,n}}{h_1^2} + \frac{u_{i,j+1}^{\varepsilon,n}-2u_{i,j}^{\varepsilon,n}+u_{i,j-1}^{\varepsilon,n}}{h_1^2}, \\ \frac{u_{i+1,j}^{\varepsilon,n}-u_{i,j}^{\varepsilon,n}}{h_1} \end{array} \right) f'\big(u_{i,j}^{\varepsilon,n}\big) \right]
$$

$$
\times \big(u_{i+1,j}^{\varepsilon,n} - u_{i,j}^{\varepsilon,n}\big)
$$

$$
- r_2 \max \left[0, a_{i,j}^2 F_2 \left(\begin{array}{l} \frac{u_{i,j+1}^{\varepsilon,n}-2u_{i,j}^{\varepsilon,n}+u_{i,j-1}^{\varepsilon,n}}{h_2^2} + \frac{u_{i+1,j}^{\varepsilon,n}-2u_{i,j}^{\varepsilon,n}+u_{i-1,j}^{\varepsilon,n}}{h_2^2}, \\ \frac{u_{i,j}^{\varepsilon,n}-u_{i,j-1}^{\varepsilon,n+1/2}}{h_2} \end{array} \right) f'\big(u_{i,j}^{\varepsilon,n}\big) \right]
$$

$$
\times \big(u_{i,j}^{\varepsilon,n} - u_{i,j-1}^{\varepsilon,n}\big)
$$

$$
- r_2 \min \left[0, a_{i,j}^2 F_2 \left(\begin{array}{l} \frac{u_{i,j+1}^{\varepsilon,n}-2u_{i,j}^{\varepsilon,n}+u_{i,j-1}^{\varepsilon,n}}{h_2^2} + \frac{u_{i+1,j}^{\varepsilon,n}-2u_{i,j}^{\varepsilon,n}+u_{i-1,j}^{\varepsilon,n}}{h_2^2}, \\ \frac{u_{i,j+1}^{\varepsilon,n}-u_{i,j}^{\varepsilon,n}}{h_2} \end{array} \right) f'\big(u_{i,j}^{\varepsilon,n}\big) \right]
$$

$$
\times \big(u_{i,j+1}^{\varepsilon,n} - u_{i,j}^{\varepsilon,n}\big),
$$

$$
u_i^{\varepsilon,0} = u^{\varepsilon,0}(ih_1, jh_2). \tag{15}
$$

4.1. Stability results

Let us now provide a stability proposition for numerical scheme (15).

Proposition 4.1.1. *Assume that a_1, a_2, F_1, and F_2 belong in $BV(\Re^2) \cap L^\infty(\Re^2)$. Under the Courant–Friedrichs–Lewy (CFL) conditions, $r_1|a_1 f' F_1| < 1/2$ and $r_2|a_2 f' F_2| < 1/2$, the above scheme is stable for the L^∞ norm and the total variation in space, as well as for the total variation in time in the Tonnelli–Cesari sense, specifically*:

$$\text{(i)} \quad \left|u_{i,j}^{\varepsilon,n}\right| \leqslant \|u_0\|_{L^\infty(\Re)}, \quad \forall i, j \in Z, \ \forall n \in \mathbb{N},$$

$$\text{(ii)} \quad \sum_{i,j\in Z} \left|u_{i+1,j}^{\varepsilon,n} - u_{i,j}^{\varepsilon,n}\right| + \left|u_{i,j+1}^{\varepsilon,n} - u_{i,j}^{\varepsilon,n}\right| \leqslant TV(u_0), \quad \forall n \in \mathbb{N},$$

$$\text{(iii)} \quad \sum_{i,j\in Z} \left|u_{i,j}^{\varepsilon,n+1} - u_{i,j}^{\varepsilon,n}\right| \leqslant TV(u_0), \quad \forall n \in \mathbb{N}.$$

Proof. Set

$$\alpha_{i,j}^n = \max\left[0, a_{i,j}^1 F_1\left(\begin{matrix}\frac{u_{i+1,j}^{\varepsilon,n} - 2u_{i,j}^{\varepsilon,n} + u_{i-1,j}^{\varepsilon,n}}{h_1^2} + \frac{u_{i,j+1}^{\varepsilon,n} - 2u_{i,j}^{\varepsilon,n} + u_{i,j-1}^{\varepsilon,n}}{h_1^2}, \\ \frac{u_{i,j}^{\varepsilon,n} - u_{i-1,j}^{\varepsilon,n}}{h_1}\end{matrix}\right) f'\left(u_{i,j}^{\varepsilon,n}\right)\right],$$

$$\beta_{i,j}^n = \min\left[0, a_{i,j}^1 F_1\left(\begin{matrix}\frac{u_{i+1,j}^{\varepsilon,n} - 2u_{i,j}^{\varepsilon,n} + u_{i-1,j}^{\varepsilon,n}}{h_1^2} + \frac{u_{i,j+1}^{\varepsilon,n} - 2u_{i,j}^{\varepsilon,n} + u_{i,j-1}^{\varepsilon,n}}{h_1^2}, \\ \frac{u_{i+1,j}^{\varepsilon,n} - u_{i,j}^{\varepsilon,n}}{h_1}\end{matrix}\right) f'\left(u_{i,j}^{\varepsilon,n}\right)\right],$$

$$\gamma_{i,j}^n = -\max\left[0, a_{i,j}^2 F_2\left(\begin{matrix}\frac{u_{i,j+1}^{\varepsilon,n} - 2u_{i,j}^{\varepsilon,n} + u_{i,j-1}^{\varepsilon,n}}{h_2^2} + \frac{u_{i+1,j}^{\varepsilon,n} - 2u_{i,j}^{\varepsilon,n} + u_{i-1,j}^{\varepsilon,n}}{h_2^2}, \\ \frac{u_{i,j}^{\varepsilon,n} - u_{i,j-1}^{\varepsilon,n+1/2}}{h_2}\end{matrix}\right) f'\left(u_{i,j}^{\varepsilon,n}\right)\right],$$

$$\lambda_{i,j}^n = \min\left[0, a_{i,j}^2 F_2\left(\begin{matrix}\frac{u_{i,j+1}^{\varepsilon,n} - 2u_{i,j}^{\varepsilon,n} + u_{i,j-1}^{\varepsilon,n}}{h_2^2} + \frac{u_{i+1,j}^{\varepsilon,n} - 2u_{i,j}^{\varepsilon,n} + u_{i-1,j}^{\varepsilon,n}}{h_2^2}, \\ \frac{u_{i,j+1}^{\varepsilon,n} - u_{i,j}^{\varepsilon,n}}{h_2}\end{matrix}\right) f'\left(u_{i,j}^{\varepsilon,n}\right)\right].$$

The numerical scheme is then rewritten as

$$\begin{aligned} u_{i,j}^{\varepsilon,n+1} = u_{i,j}^{\varepsilon,n} &- r_1\alpha_{i,j}^n\left(u_{i,j}^{\varepsilon,n} - u_{i-1,j}^{\varepsilon,n}\right) - r_1\beta_{i,j}^n\left(u_{i+1,j}^{\varepsilon,n} - u_{i,j}^{\varepsilon,n}\right) \\ &- r_2\gamma_{i,j}^n\left(u_{i,j}^{\varepsilon,n} - u_{i,j-1}^{\varepsilon,n}\right) - r_2\lambda_{i,j}^n\left(u_{i,j+1}^{\varepsilon,n} - u_{i,j}^{\varepsilon,n}\right). \end{aligned}$$

Using the CFL condition, we have

$$\alpha_{i,j}^n \geqslant 0 \quad \text{and} \quad \left|r_1\alpha_{i,j}^n\right| \leqslant \frac{1}{2},$$
$$\beta_{i,j}^n \leqslant 0 \quad \text{and} \quad \left|r_1\beta_{i,j}^n\right| \leqslant \frac{1}{2},$$
$$\gamma_{i,j}^n \geqslant 0 \quad \text{and} \quad \left|r_2\gamma_{i,j}^n\right| \leqslant \frac{1}{2},$$
$$\lambda_{i,j}^n \leqslant 0 \quad \text{and} \quad \left|r_2\lambda_{i,j}^n\right| \leqslant \frac{1}{2}.$$

The rest of the proof is similar to the one-dimensional case. □

Once again along the same lines as in the one-dimensional case, we can establish a convergence result in the sense defined therein.

4.2. Tests and discussion

Several tests were performed to measure the effectiveness of the proposed explicit numerical scheme, as well as that of the model. We began by working with blurred or noisy synthetic images and real blurred images, and then used real scene images (no noise added) taken from the Web. In this section, we comment on the results we obtained.

In all our tests, we set $r = 0.8$, $a \equiv 1$, $f(u) = (1/2)u^2$, $F(u, v) \equiv 1$, and $a \equiv \text{sign}(\Delta u^0)\,\text{sign}(u_x^0)$. The images were normalized to belong in the interval $[0, 1]$ in order to avoid a strict CFL condition and cause the process to slow down. As in the one-dimensional case, the KCS mollifier was used in the regularization process for the original images.

The first test involved blurry (Fig. 3a) and noisy (Fig. 3b) synthetic images representing a disc and a square. The results were obtained by taking $h(\varepsilon) = 1.5$ for the first test and $h(\varepsilon) = 6$ for the second. We can see that the image is perfectly restored in both cases.

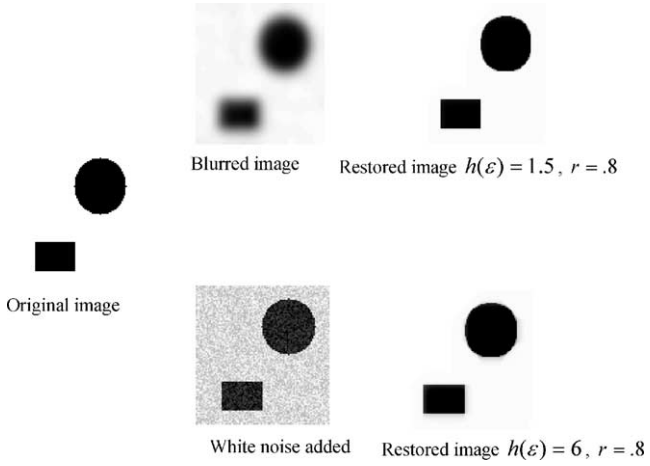

Fig. 3. Tests on a synthetic image.

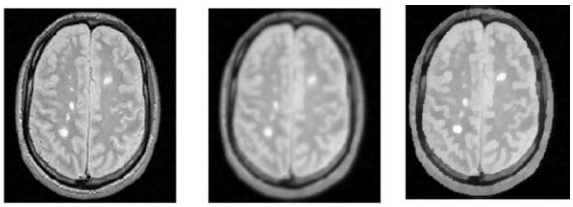

Fig. 4. Test on a blurred real image using a convolution with a Gaussian ($\sigma = 4$).

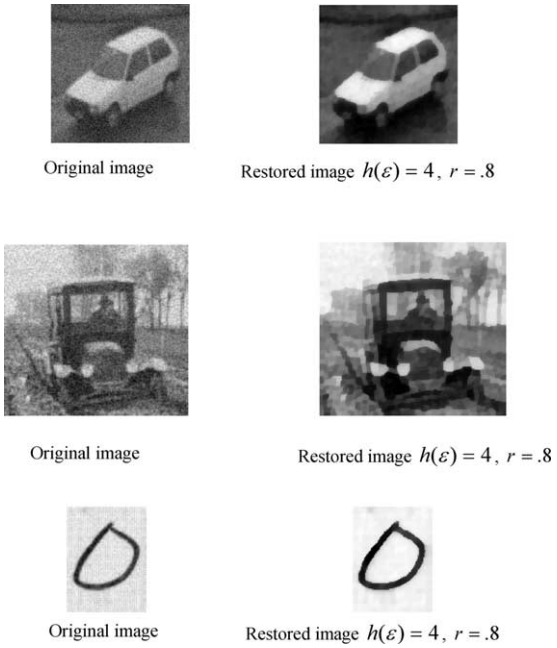

Fig. 5. Tests on real scenes without added blurring or noise.

The second test consisted in blurring real scenes of the brain (Fig. 4). The results obtained after seven iterations are highly satisfactory. The last test consisted in restoring and enhancing real scene images (Fig. 5). The image of the automobile was taken from the Web, and the digit zero was taken from a database from Suny Buffalo (CEDAR). No noise was added to either image. Here again, the results obtained after only seven iterations are quite conclusive.

Remark. By interpreting the model within the framework of the generalized functions algebra, we are dealing with representatives, which are smooth functions. This means that the original signal is smoothed and then almost all noise is removed at the beginning of the process. Also note that such models do not use any a priori information regarding the noise.

5. Conclusion

In Part I of this paper, we presented a generalized (for one- and two-dimensional cases) shock model for signal enhancement and restoration. A detailed theoretical study of the models in the framework of the generalized functions algebra is also provided. In Part II of this paper, we proposed a stable, explicit and efficient numerical scheme derived from the models proposed in Part I to enhance and restore signals. Promising results in both the one- and two-dimensional cases that demonstrate the enhancement and restoration performance of the derived schemes are presented, as well as the positive impact of controlling the shock speed on processing time.

Acknowledgments

This work was supported by research grants received from NSERC (The Natural Sciences and Engineering Research Council of Canada) and FCAR (La Fondation du Conseil et Aide à la Recherche du Québec).

References

[1] L. Alvarez, P.L. Lions, J.M. Morel, Image selective smoothing and edge detection by nonlinear diffusion (ii), SIAM J. Numer. Anal. 29 (1992) 845–866.
[2] L. Alvarez, L. Mazorra, Signal and image restoration using shock filters and anisotropic diffusion, SIAM J. Numer. Anal. 31 (1994) 590–605.
[3] S. Bernard, J.F. Colombeau, A. Meul, L. Remaki, Conservation laws with discontinuous coefficients, J. Math. Anal. Appl., accepted.
[4] J.F. Colombeau, Multiplication of Distribution, in: Lecture Notes in Mathematics, Vol. 1532, Springer-Verlag, 1992.
[5] E. Godlewski, P.A. Raviart, Hyperbolic systems of conservation laws, SMAI 3/4 (1991).
[6] J.J. Koenderink, The structure of images, Biol. Cybernet. 53 (1984) 363–370.
[7] S. Osher, L. Rudin, Feature oriented image enhancement using shock filters, SIAM J. Numer. Anal. 27 (1990) 919–940.
[8] L. Remaki, Étude théorique et numérique des équations quasi-linéaires à coefficients discontinus et acoustique linéaire 2D, Ph.D. thesis, Université Claude Bernard Lyon 1, Lyon, France, 1997.
[9] L. Remaki, M. Cheriet, KCS—new kernel family with compact support in scale space: formulation and impact, IEEE Trans. Image Process. (1999), in press.
[10] L. Rudin, Shock filters, in: Rockwell International Science Center Annual DARPA T.R., 1984.